

---

# Finite Element Analysis Coupled with Feedback Control for Dynamics of Metal Pushing V-Belt CVT

---

Toshihiro Saito

Additional information is available at the end of the chapter

<http://dx.doi.org/10.5772/46194>

---

## 1. Introduction

Nowadays automobiles are required to meet environmental requirements, such as lower exhaust emissions and higher fuel economy. One of the key factors for improving the overall efficiency of a vehicle is the efficiency of its transmission.

A CVT has a greater potential for improving fuel economy than a step-type automatic transmission (AT), because of its integrated control with the engine [1]. That is, CVTs are capable of continuously tracing engine operating ranges with high fuel efficiency. Another advantage is that CVTs allow vehicles to drive without lowering the driving torque or the engine rpm while shifting the gear ratio.

However, when the transmission efficiency of a CVT by itself is compared with a step-type AT, CVT is known to have lower efficiency because its driving torque is transferred by means of contact and friction [2]. The transmission efficiency of a CVT is determined by friction loss at its oil pump and metal pushing V-belt. The oil pump must produce enough pulley pressure so that the metal V-belt mounted between two pulleys does not slip. A higher pulley pressure, however, means a greater friction loss at the oil pump [3].

As for the metal V-belt, gradually lowering pulley pressure while maintaining a constant transmission torque increases the transmission efficiency of the belt by itself, as long as it does not slip on the pulleys. However, the transmission efficiency begins to drop under a certain operating condition. This implies the existence of an optimum operating condition that maximizes the transmission efficiency of the belt [4]. To find this condition, it is important to predict friction loss at each portion of the metal V-belt during CVT operation.

A considerable amount of research has so far been made on methods for calculating friction loss that occurs at each part of the V-belt, but many of them use simple equations that are

based on assumptions and not linked with dynamic belt behavior [5]. Accordingly, although these methods simulate the tendency of friction loss on each belt part, they are not sufficient for examining the influence on friction loss of metal belt shape and pulley rigidity.

A commercially available multi-body simulation (MBS) code used to be chosen for the dynamic belt behavior [7]. In the MBS model, each V-belt block was treated as a separate rigid body. Contact normal forces were modeled between adjacent blocks, using realistic stiffness and damping properties. Contact normal forces, along with both radial and circumferential friction forces, were also modeled between the block edges and pulley faces. Block geometry and material properties were used to arrive at contact stiffness and damping characteristics. As such, the MBS model contained a relatively small number of degrees of freedom. At the results, the contact forces between the block edges and pulley faces could be only obtained, not the contact pressure distribution.

Therefore, the following describes how CVT-ratio control logic was included in the previously reported technology for simulating the dynamic behavior of a metal pushing V-belt, and presents how the new simulation can closely reproduce actual operation. Thus, this paper reports a technology developed to predict the transmission efficiency of a CVT drive system comprising a metal pushing V-belt and pulleys.

## 2. Development aims

### 2.1. Maintaining speed ratio with feedback control

Figure 1 shows the main section of the CVT used in this development. A metal V-belt is mounted in the V groove on two pulley shafts, and a pair of movable pulleys are mounted on the shafts to face each other. The movable pulleys are shifted in the axial direction by line oil pressure supplied from the inside of the shaft. When the CVT is in operation, feedback control is exercised to maintain an arbitrary speed ratio between the two pulleys, varying the oil pressure applied to the large-diameter (in terms of belt mounting position) pulley while maintaining a constant pressure for the small-diameter pulley. When taking an example of the top ratio, the drive pulley speed, driven pulley torque, driven pulley oil pressure, and target ratio are input to the feedback control system. The system then outputs the driven pulley speed, drive pulley torque, and drive pulley oil pressure. The input-output relation differs from the metal V-belt behavior simulation technology developed previously, so it was necessary to incorporate a new feedback control into the simulation in this project.

### 2.2. Pulley shaft thrust load ratio

Pulley shaft thrust load is obtained as the sum of two values: the product of oil pump line pressure and its acting area, as well as the product of centrifugal oil pressure and its acting area. The ratio between drive pulley thrust load and driven pulley thrust load, referred to as the pulley shaft thrust load ratio, has a positive correlation with the speed ratio; therefore, this ratio is uniquely determined once the speed ratio is set. Because the developed simulation outputs pulley shaft thrust loads, its prediction accuracy can be verified by comparing simulated and measured values.

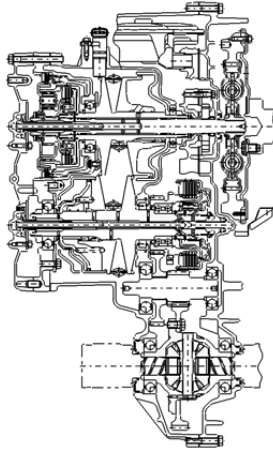


**Figure 1.** CVT cross section

### 2.3. Transmission efficiency

Transmission efficiency can be obtained by multiplying the ratio between drive shaft torque and driven shaft torque by the speed ratio, as expressed in Equation (1). Here, each torque value can be obtained as the product of a tangential friction force, generated between the V-face of each pulley and metal V-belt elements, and the effective element V-surface radius. As such, it is necessary to accurately predict the direction of a friction force acting on each element V-surface and its effective radius under that condition. The effective radius of the element V-surface is influenced by its contact pressure distribution. This means that it is also necessary to consider the elastic deformation of the element V-surface.

For this reason, to simulate the transmission efficiency of the metal pushing V-belt, the following were set as development objectives:

1. Implement feedback control equivalent to speed ratio control performed in an actual vehicle
2. Quantify sliding velocities and friction forced at various element contact areas
3. Calculate friction losses at various portions of the metal V-belt

## 3. Technology of predict transmission efficiency of metal pushing V-belt

### 3.1. V-belt model consideration of element deformation

The transmission efficiency of a metal pushing V-belt is mainly determined by friction losses that occur between its elements and pulleys and between the elements and rings. Friction loss has a correlation with the product of the friction force and sliding velocity of a friction surface. Accordingly, a key to predicting the transmission efficiency is to simulate the friction forces and sliding velocities of the element V surfaces in contact with the pulley. These friction forces and sliding velocities have distributions on the pulley, and these

distributions cannot be simulated accurately unless element deformation is taken into account (Figure 2). Because the effective radius of elements would be influenced by the contact pressure distribution. For this reason, an element stress prediction model [6] previously designed to consider element deformation was modified to make a model of the metal V-belt used in this study.

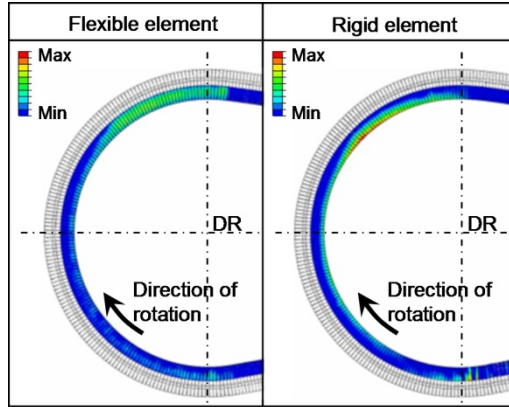


**Figure 2.** Comparison of friction force distribution of Element V-surfaces on DR pulley

Figure 3 and Figure 4 show the model. Two flexible solid elements are employed in the direction of thickness for individual elements to reproduce bending deformation. Three flexible solid elements are used to divide the R section of the element neck, where stress is thought to concentrate. Reproduction of detailed form of the nose and hole sections has been prioritized, and therefore modeled with rigid elements. Four flexible shell elements have been used in the direction of width to model each layer of rings to enable reproduction of the crowning of the rings. In addition, the ring-element, element-element, ring-ring and element-pulley contact surfaces have been defined, and appropriate friction characteristics have been assigned in each case.

To make the load conditions around the belt pulleys closely resemble the layout in an actual CVT, beam elements were used to express the shafts. In this model, the shafts are supported at the bearing positions. Also, a gear is provided to mesh with the driven (DN) shaft to reflect reaction forces applied by the gear. Because the belt mounting diameter varies depending on speed ratios, deflection rigidity calculated for the mounting positions of each ratio was applied to the pulley V-face. Regarding the relation between each shaft and the movable pulley, the model defines a fitting clearance at their engagement position, as well as a backlash in the rotational direction at the roller position.

Figure 5 shows the flow of analyzing the metal V-belt. In this flow, the belt is initially placed at the perfect-circle position under no stress, and then both pulleys are moved to a specified shaft distance. Next, misalignment is applied to one of the pulleys. Then, the drive pulley is gradually accelerated to reach a target speed, while pulley thrust pressure is being applied. In the meantime, reverse torque is gradually applied to the driven pulley.

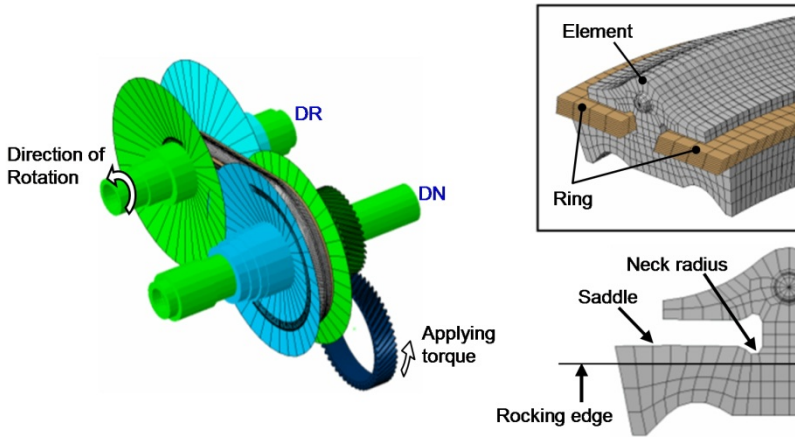


Figure 3. Metal V-belt model for predicting transmission efficiency considering shaft deformation

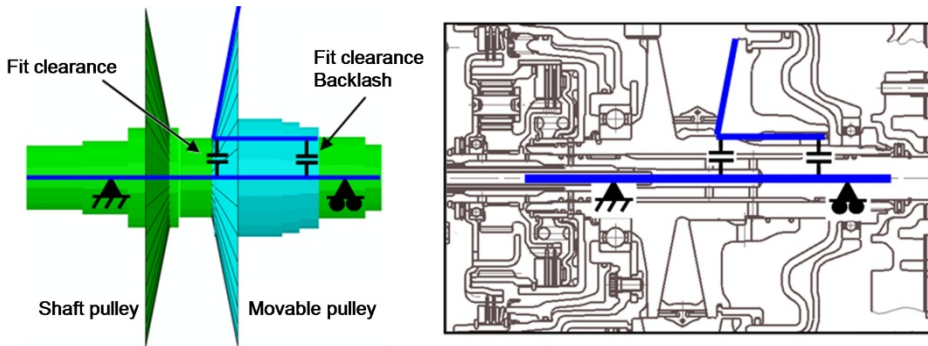


Figure 4. Boundary condition around pulley shaft

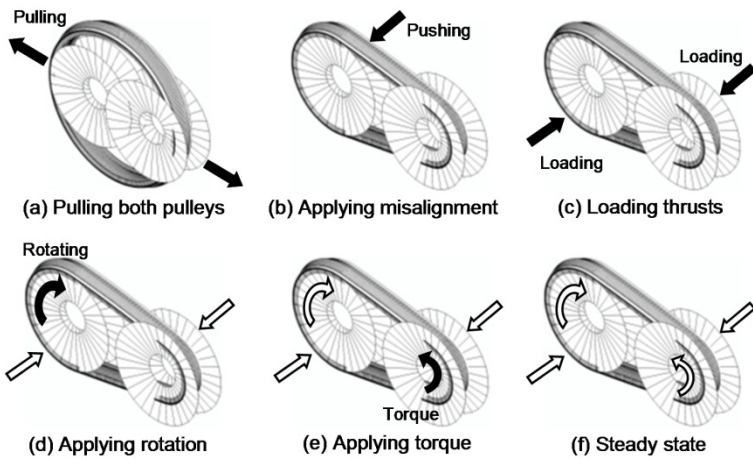


Figure 5. Analytic procedure

### 3.2. Belt transmission efficiency prediction using pulley thrust pressure control

The transmission efficiency  $\eta$  of the V-belt can be obtained by the following equation:

$$\eta = \frac{\omega_{dn} \times T_{dn}}{\omega_{dr} \times T_{dr}} = i \frac{T_{dn}}{T_{dr}} \tag{1}$$

- $\omega_{dr}$  : drive (DR) shaft speed
- $\omega_{dn}$  : driven (DN) shaft speed
- $i$  : ratio
- $T_{dr}$  : DR shaft torque
- $T_{dn}$  : DN shaft torque

Thus, the DR shaft torque, DN shaft torque, and ratio must be obtained to predict efficiency  $\eta$ . The conventional element stress prediction model required simulations to be made based on pulley thrust pressures measured in an actual CVT. Unlike element stress measurement, the transmission efficiency can be easily measured in an actual vehicle, but it would be impractical for a simulation to require actual measurements to predict the efficiency. Accordingly, a pulley thrust controller used in the previous research [7] was implemented in the simulation to apply pulley thrust pressure that depended on each operating condition.

Figure 6 is a block diagram of the thrust controller. Enclosed in the dashed box in this figure is a traditional proportional-integral (PI) controller. This controller calculates the actual ratio from  $\omega_{dr}$  and  $\omega_{dn}$  of the belt model, and adjusts pulley thrust pressure by means of a feedback loop until the ratio reaches a target value  $I_{target}$ . Controller gains were re-defined because the previous metal V-belt model was replaced with the element stress prediction model.

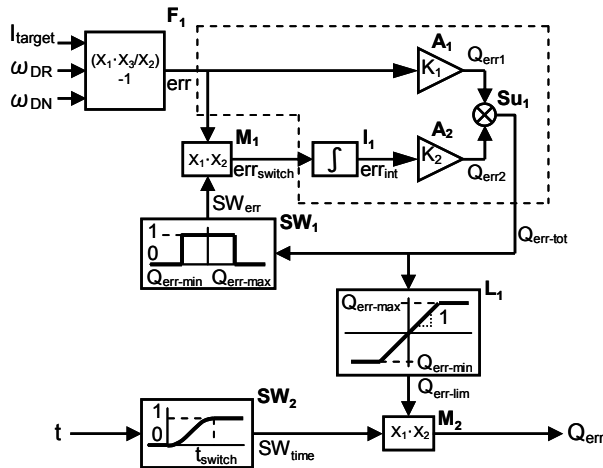


Figure 6. Thrust controller block diagram

Figure 7 shows calculations made with the metal V-belt model incorporating the above pulley thrust pressure control. In this simulation,  $\omega_{dr}$ ,  $T_{dn}$ , and the driven pulley thrust

pressure  $Q_{dn}$  were given as input, and the drive pulley thrust pressure  $Q_{dr}$  was controlled to make the actual ratio reach the target value. Because speed ratio error must be considered in deciding the  $Q_{dr}$  control value, pressure was applied before starting the rotation. Then, ratio control was started after making sure that the actual ratio had been read accurately. As demonstrated in Figure 7, the speed ratio is maintained at the target value when the pulley thrust pressure is controlled by the ratio controller.

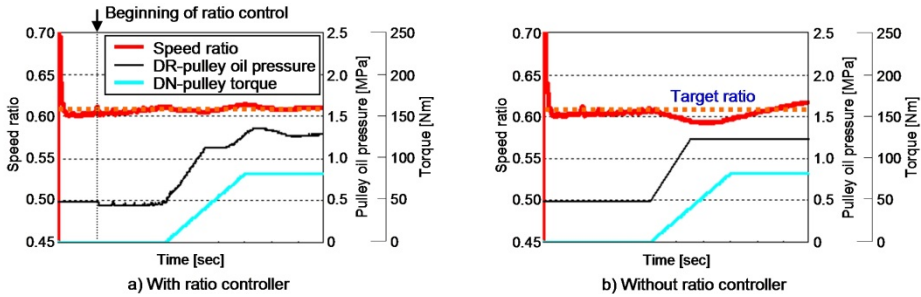


Figure 7. Effect of ratio controller

Figure 8 shows the belt transmission efficiency obtained from the computation result of this model. As shown here, the simulation implementing pulley thrust pressure control enables transmission efficiency prediction at a target speed ratio.

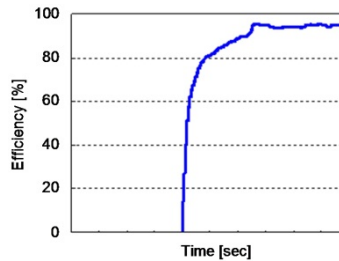


Figure 8. Calculated transmission efficiency of metal V-belt with ratio controller

## 4. Belt transmission efficiency at different ratio

In a CVT equipped with a metal pushing V-belt, the transmission efficiency is known to peak at the speed ratio of 1.0 (MID). The efficiency lowers gradually while a vehicle is decelerating (shifting to LOW) or accelerating (shifting to OD). The developed simulation was used to calculate friction loss at each portion of the metal V-belt at different speed ratios.

### 4.1. Accuracy of belt efficiency prediction

Figure 9 shows belt transmission efficiency calculated for and measured at the MID, LOW, and OD ratios under a certain operating condition. Figure 10 shows the calculated and

measured pulley shaft thrust load ratios. Both graphs indicate the same tendency, which verifies the validity of simulations at all ratios.

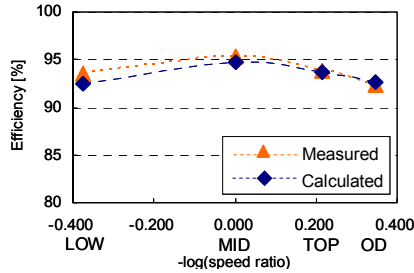


Figure 9. Belt transmission efficiency

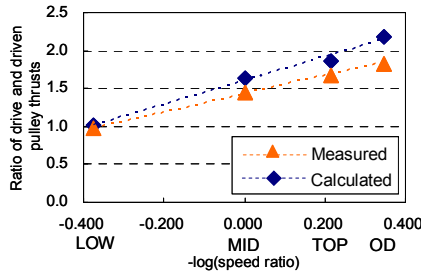


Figure 10. Ratio of drive and driven pulley thrusts

#### 4.2. Friction loss of metal V-belt at each ratio

As mentioned before, the transmission efficiency of a metal pushing V-belt is mostly determined by friction loss that occurs between its elements and pulleys and between the elements and rings. Calculations were therefore made to compare friction losses of these areas at different ratios.

Figure 11 shows friction forces acting on the element V-surface and the element-pulley speed difference during one rotation of the belt. Similarly, Figure 12 shows friction forces acting on the element saddle surface and the element-ring speed difference. Both friction forces and speed differences are in the torque transmission direction. The speed difference is calculated for the same belt mounting position at each ratio. Figure 11 shows the speed difference between the element V-surface speed and the pulley speed, and Figure 12 the difference between the element saddle speed and the speed of the innermost ring.

When a speed difference occurs between two parts to which a friction force is applied, this speed difference may be assumed to be sliding velocity. Thus, friction loss can be obtained by multiplying the sliding velocity and the friction force. Figure 13 shows friction losses calculated in this way for the element V-surface and the saddle surface at each ratio. When attention is paid to friction loss on the element V-surface, loss is large near the drive pulley exit at the LOW ratio. In contrast, at the MID and OD ratios, friction loss is greater at the



pulley entrance. On the driven pulley, loss is greater near the pulley exit, regardless of the ratio. When studied in relation to sliding velocity, friction loss becomes greater at locations where the sliding velocity is higher at all three ratios.

As for friction loss on the saddle surface, loss is smaller at the MID ratio than the other ratios. This is because, at the MID ratio, the belt mounts on a medium-diameter position on the pulley, where the sliding velocity between the pulley and the element is lower. At the other ratios, friction loss on the saddle surface is greater when it is on the smaller-diameter pulley.

A similar comparison was made with friction loss that occurs between adjacent elements and between adjacent of rings (Figure 14, Figure 15, and Figure 16).

As shown in each figure, friction loss is smaller than the loss calculated for the two aforementioned areas. This is because the sliding velocity is smaller between adjacent elements and adjacent rings where a friction force is present.

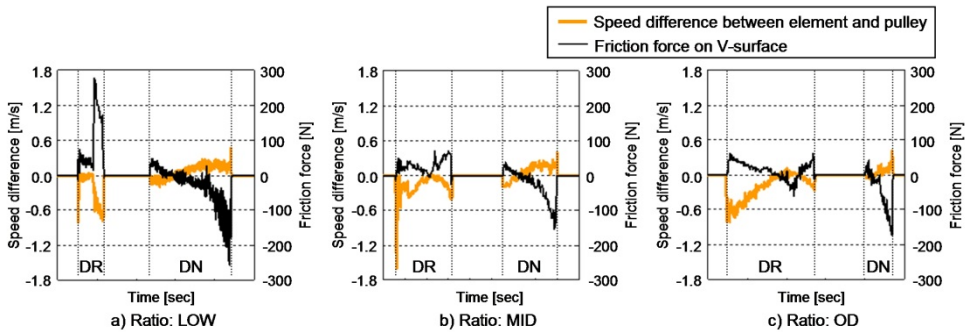


Figure 11. Element V-surface friction force and element-pulley speed difference

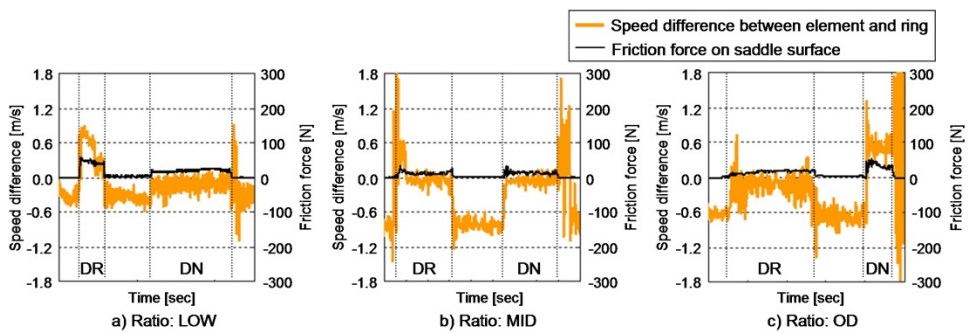


Figure 12. Element saddle-surface friction force and element-ring speed difference

Figure 17 shows the comparison of friction losses per unit time at the three speed ratios. When this figure is studied with Figure 9, it is clear that friction loss is greater at ratios with

lower transmission efficiency. The comparison also reveals that the transmission efficiency is affected by friction losses on the element V surface and the saddle surface. When attention is paid to the proportion of friction losses at different ratios, friction losses on the element V-surface and the saddle surface are almost equal at the LOW ratio. At the OD ratio, friction loss on the saddle surface accounts for a dominant proportion.

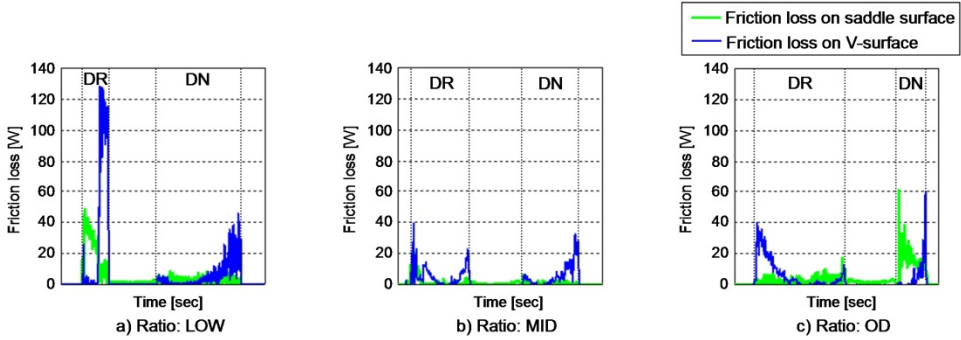


Figure 13. Friction loss on element friction surface

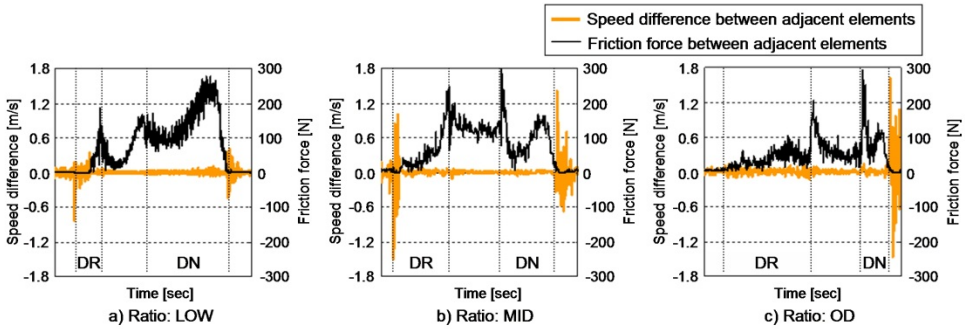


Figure 14. Friction force and speed difference between adjacent elements

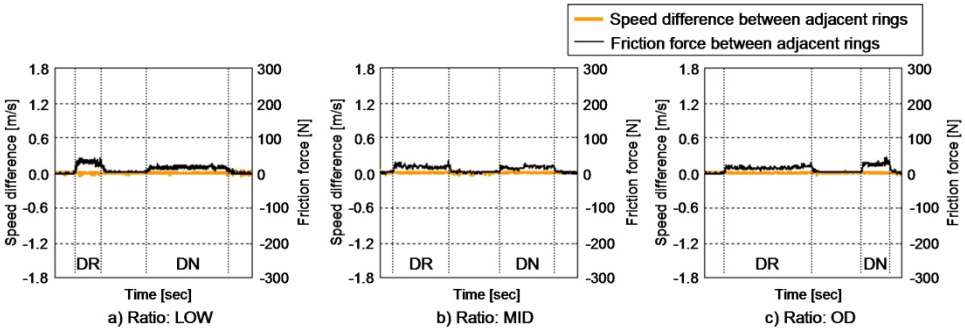


Figure 15. Friction force and speed difference between adjacent rings

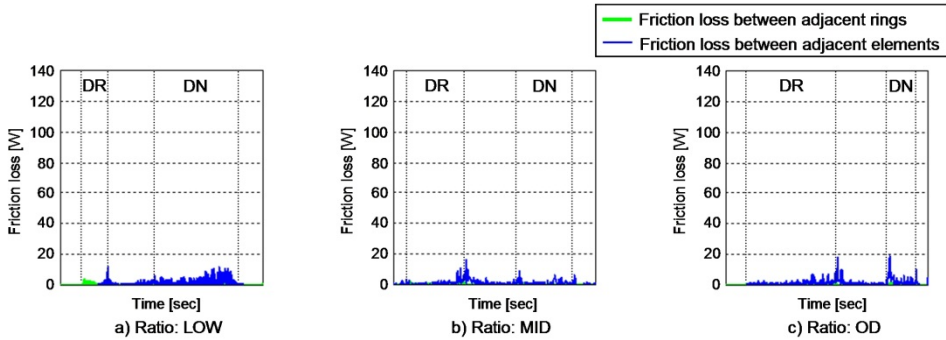


Figure 16. Friction loss between adjacent elements and between adjacent rings

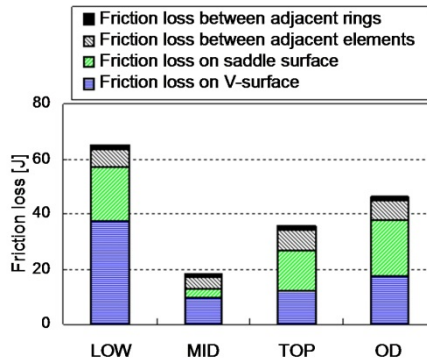
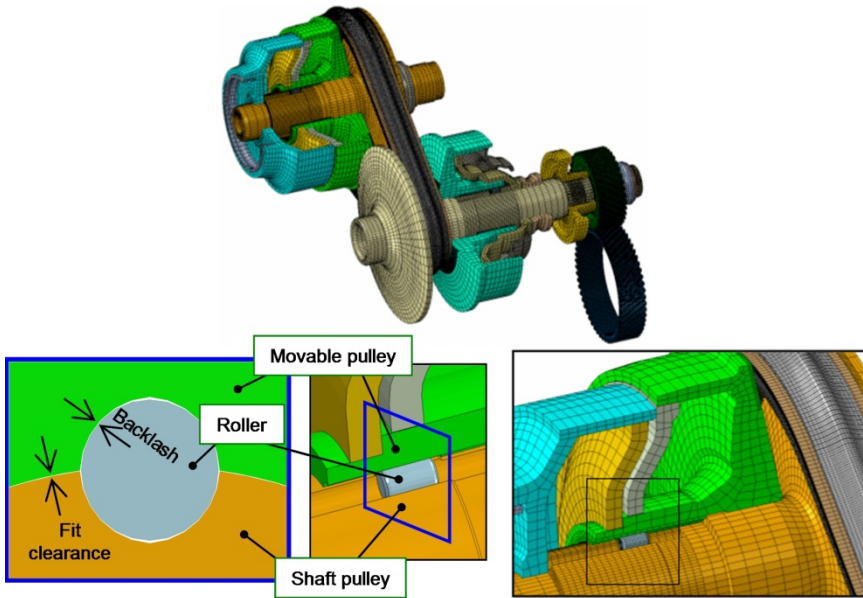


Figure 17. Belt friction loss per unit time

### 5. Application for actual CVT configuration

Figure 18 shows an actual CVT configuration to be calculated the transmission efficiency. Replacement of the former single-piston configuration with double pistons aligned in the axial direction has resulted in approximately 1.8 times more thrust at identical oil pressures. This has reduced line pressure when the CVT is in its frequently used overdrive ratio, thus reducing the pump workload. In this mode, the elements and the pulleys are modeled as elastic bodies to help enable their deformation to be considered. The number of divisions in the circumferential direction was increased and a coefficient of friction was set to help enable study of the effect of the fit clearance of the fitted parts of the pulley shaft and the movable pulley and of the roller spline backlash. Figure 19 shows Von Mises stress distribution except the gears. Most of the parts are now modeled as flexible bodies.

The transmission efficiency is now predicted using pulley thrust pressure control with appropriate control gains. (Figure 20) The speed ratio is kept at a target speed ratio during this simulation.



Pulley fit clearance and backlash

Figure 18. Metal V-belt model considering pulley V-surface deformation

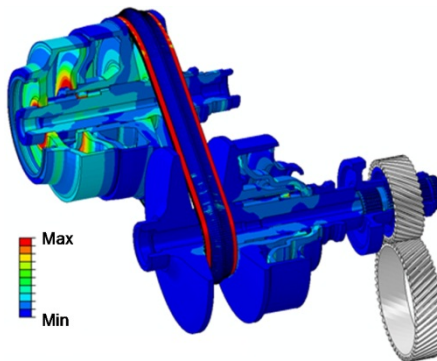


Figure 19. Stress distribution of Metal V-belt and pulleys

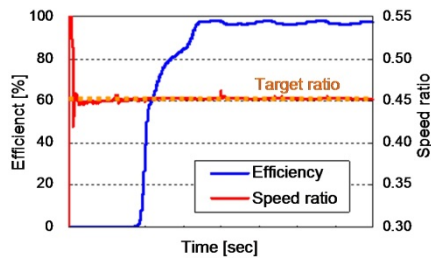


Figure 20. Calculated transmission efficiency of metal V-belt with FEM pulleys

### 5.1. Effect of fit clearance on transmission efficiency

In CVTs equipped with metal pushing V-belts, transmission efficiency is known to peak at the shift ratio of 1.0 (MID). Transmission efficiency declines gradually while the vehicle is decelerating (shifting to LOW) or accelerating (shifting to OD). However, the effect of the clearance of the section in which the external shape of the pulley shaft and the internal diameter of the movable pulley are in contact and of the roller on the transmission efficiency and the strength of the metal pushing V-belt is not necessarily clear. The method discussed here was therefore employed, using the OD ratio, in order to calculate friction loss for each part of the belt when the clearance of the section in which the external shape of the pulley shaft and the internal diameter of the movable pulley are in contact (“large-diameter clearance” below) and the clearance in the direction of rotation determined by the roller (“backlash” below) were varied.

Figure 21 and 22 show that when the large-diameter clearance of the fitted sections becomes narrower, friction loss on the element V-surfaces is reduced, and the transmission efficiency of the belt increases. Fig. 23 shows the changes in the winding diameter of the belt at this time. When the large-diameter clearance increases, the changes in the belt winding diameter also increase in magnitude. In other words, the belt slips in the radial direction, thus reducing the amount of friction force available for transmission, with the result that transmission efficiency declines. In addition, a comparison of the surface pressure distribution on the element V-surfaces shows that when the large-diameter clearance becomes greater, the surface pressure distribution tends towards the inside of the radius (Fig. 24). This is believed to be an effect of the fact that when the belt is transmitting torque, its effective radius is reduced, and torque transmission efficiency declines.

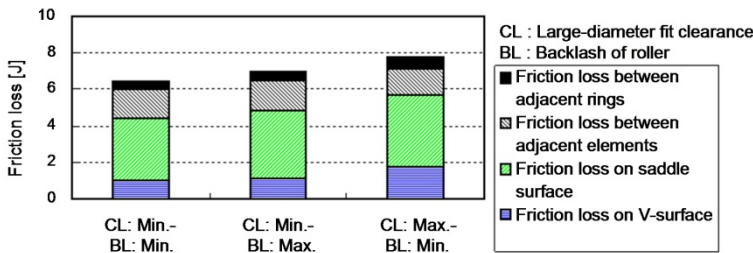


Figure 21. Fit clearance and friction loss on belt surface

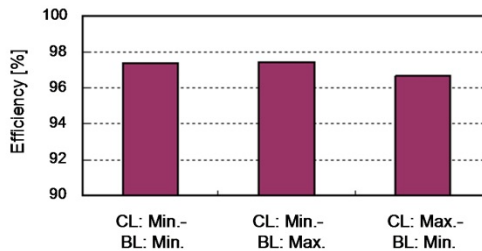


Figure 22. Fit clearance and belt transmission efficiency

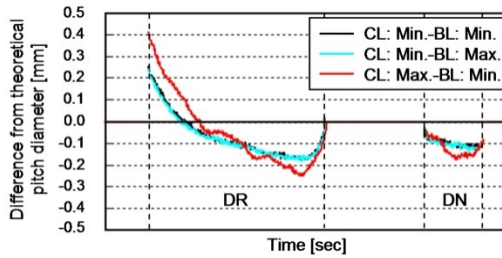


Figure 23. Fit clearance and belt pitch diameter

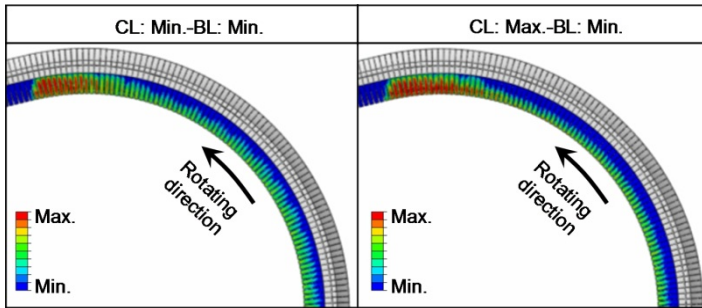


Figure 24. Fit clearance and distribution of element V-surface pressure

**5.2. Effect of pulley stiffness on belt transmission efficiency**

Of the parts that make up a CVT, the size and weight of the pulleys is particularly high, creating the need for the development of lighter-weight pulleys. Effects on the strength of metal pushing V-belts due to changes in pulley stiffness resulting from reduction in weight have also been reported [5,7]. As in the analyses conducted in the previous chapters, the effect on the transmission efficiency and strength of the belt when the pulley stiffness was varied was therefore considered. Altering the form of the pulleys in order to quantitatively vary stiffness would represent a challenge, and Young’s modulus for the pulleys in the model discussed above was therefore altered in order to vary the stiffness. The Young’s modulus of the pulleys was varied by  $\pm 20$  against Young’s modulus for iron, and the fit clearance was minimized.

As Figure 25 and 26 show, when the pulley stiffness is reduced, friction loss on the element V-surfaces increases, and the transmission efficiency of the belt declines. Figure 27 shows changes in the winding diameter of the belt at this time. A comparison of these results with the results of former chapters shows that the effect produced by reducing the stiffness of the pulleys displays an identical tendency to that produced by increasing the fit clearance, but the magnitude of the change is smaller.

**6. Discussion**

These analyses focus on the steady state response under some operating conditions. However, some results show the vibration, such as speed difference between element and ring in Figure



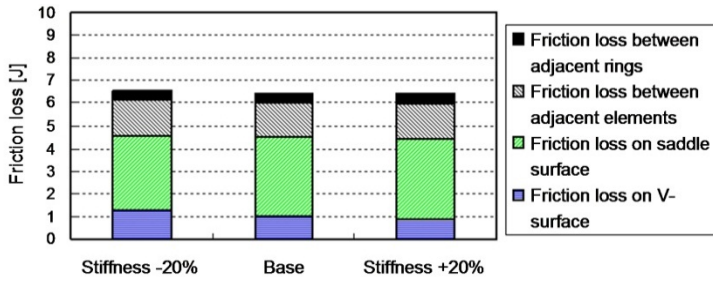


Figure 25. Pulley stiffness and friction loss on belt surface

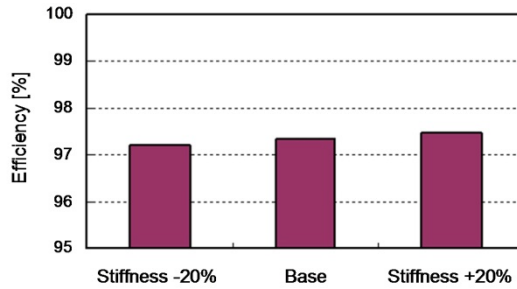


Figure 26. Pulley stiffness and belt transmission efficiency

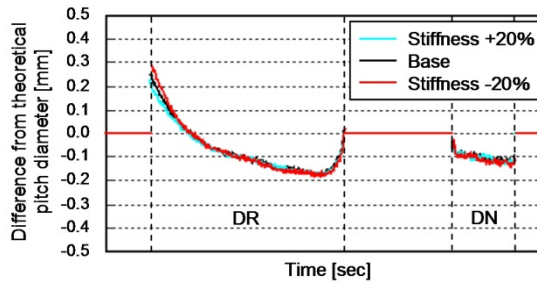


Figure 27. Pulley stiffness and belt pitch diameter

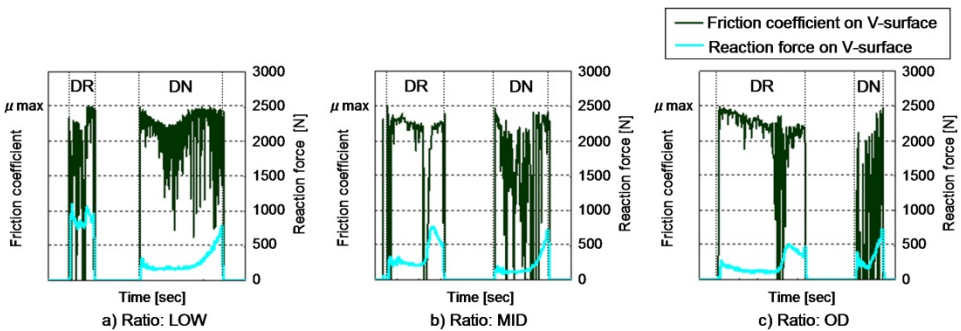


Figure 28. Friction coefficient currently used on element V-surface

12. These are two reasons for the vibration. One is the impact forces are generated when the element gets into and out the pulleys. Another is the each element behavior itself. Figure 28 shows the element reaction force on V-surface and the friction coefficient on V-surface. The friction coefficient in these analyses shows the vibration in the pulleys. This presents that each element could move individually to keep the contact and friction for adjacent parts.

## 7. Conclusion

1. Feedback control to maintain speed ratios in an actual CVT has been implemented in a metal V-belt behavior simulation, making it possible to predict the CVT transmission efficiency under an arbitrary operating condition.
2. This simulation has successfully quantified sliding velocities and friction forces of element contact areas along the entire length of the V-belt.
3. The simulation was used to calculate friction losses from sliding velocities and friction forces at different ratios—loss on the V-surface, loss on the saddle surface, loss between elements, loss between rings, and their proportions.
4. The simulation technique was also available for actual CVT configuration to predict the transmission efficiency using flexible pulley components.

## Author details

Toshihiro Saito  
*Honda R&D Co., Ltd. Automobile R&D Center, Japan*

## 8. References

- [1] Yamamoto, K., Sakaguchi, S., Kishida, M., Kimura, E. and Abe, H. "Development of Integrated Engine-CVT Control System," Honda R&D Technical review, Vol. 11, No. 1
- [2] Akehurst, S., Vaughan, N. D., Parker, D. A. and Simner, D. "Modelling of loss mechanisms in a pushing metal V-belt continuously variable transmission. Part 1: torque losses due to band friction," Proc. Instn Mech. Engrs vol. 218 Part D: J. Automobile Engineering
- [3] Veenhuizen, P. A., Bonsen, B., Klaassen, T.W.G.L., Albers, P.H.W.M., Changenet, C. and Poncy, S. "Pushbelt CVT efficiency improvement potential of servo-electromechanical actuation slip control," 2004 CVT Congress
- [4] Van der Noll, E., Van der Sluis, F., Van Dongen, T. and Van der Velde. A. "Innovative Self-optimising Clamping Force Strategy for the Pushbelt CVT," SAE Paper, 2009-01-1537
- [5] Narita, K. and Priest, M. "Metal-metal friction characteristics and the transmission efficiency of a metal V-belt-type continuously variable transmission," Proc. IMechE vol.221 Part J: J. Engineering Tribology
- [6] Saito, T. "Application of Stress Simulation Under Transient Condition for Metal Pushing V-belt of CVT," SAE Paper, 2008-01-0415
- [7] Saito, T. and Lewis, D. A. "Development of a Simulation Technique for CVT Metal Pushing V-belt with Feedback Control," SAE Paper, 2004-01-1326